Catalytic Oxidation of 2-Chlorophenol in Confined Channels of ZSM-48

Kuen-Song Lin and H. Paul Wang*

Department of Environmental Engineering, National Cheng Kung University, Tainan City, Taiwan 70101, R.O.C.

Received: December 6, 2000; In Final Form: February 23, 2001

Experimentally, the formation of undesired heavy polycyclic aromatic hydrocarbons (PAHs) and chlorinated phenol byproducts in the supercritical water oxidation (SCWO) of 2-chlorophenol (2CP) catalyzed by CuO/ZSM-48 at 673 K was significantly reduced. The reduction was attributed to the byproduct shape selectivity of the confined ZSM-48 channels. Speciation of active copper species in ZSM-48 was studied by X-ray absorption near edge structural (XANES) and extended X-ray absorption fine structural (EXAFS) spectroscopies, which suggested the existence of $(Cu_3O_2)_n$ ($n_{max} = 150$, cross section of about 1.9 Å) clusters in the channels of ZSM-48 (5.3−5.8 Å). The diffusion coefficients of the copper-oxide cluster (determined by low-temperature electron paramagnetic resonance (EPR) spectroscopy) were greater than that of the tight-fit 2CP in the channels of ZSM-48 by at least three orders. Since the catalytic SCWO of 2CP was extremely fast, we consider the possibility that copper-oxide clusters were relatively mobile if compared with the 2CP in the confined channels of ZSM-48.

Introduction

2-Chlorophenol (2CP) is a very toxic and poorly biodegradable priority pollutant.[1,2] Trace toxic byproducts such as PAHs, dioxins, and furans are frequently found in the incineration of 2CP.[3−5] Polycyclic aromatic hydrocarbons with two or more fused benzene rings in linear, angular, or cluster arrangements may be formed in the processes of pyrolysis, incomplete combustion, or carbonization of organics.[3] Many heavy PAHs are very toxic and considered carcinogenics or mutagenics.[3,4] Chlorine atoms may accelerate the abstraction of aromatic H from PAH molecules that are activated for further mass growth of PAHs to form soot eventually.[3−5] In previous studies, we found that the formation of toxic byproducts was significantly reduced due to an effective abstraction of Cl from 2CP by metal cations in supercritical water.[6,7] Precipitation of metal chloride was found in the SCWO process.[6,7] It should be noted that from an environmental viewpoint, a maximum destruction and removal efficiency (DRE) and a minimum of undesired byproducts formed in the toxic matters destruction processes are of great importance.[1−5]

The presence of a single phase and high temperatures in supercritical water ($T > 647.3$ K, $P > 217.6$ atm) allows the oxidation to proceed rapidly by an elimination of the potential interface mass transport limitations.[8,9] The desired DRE (> 99.99%, generally) of hazardous organic compounds in the supercritical water oxidation (SCWO) processes may be achieved in seconds or minutes.[10−15] However, because of the drawbacks of high-temperature and high-pressure operational conditions in the SCWO process, oxidation catalysts such as Cr_2O_3, MnO_2/CeO_2, CuO/ZnO, or CuO/ZSM-5 have been studied widely.[6,7,16−21]

Because of the unique pore systems, zeolites have excellent shape selectivities in catalytic reactions.[22−24] Zeolite ZSM-48 possesses a unidimensional channel structure based on the ferrierite sheet with linear noninterpenetrating 10-membered ring channels (with pore size of 5.3−5.6 Å running perpendicular to the sheet).[22,24] Due to the confined environment in the channels of zeolite ZSM-48, formation of high-molecular weight byproducts would be very limited. The nature of catalytic active species in the channels of ZSM-48, especially in the catalytic SCWO, has not been studied extensively.[7] Thus, the main objective of the present work was to study the speciation of copper oxides in the channels of ZSM-48 in the SCWO of 2CP by spectroscopic methods such as EXAFS, XANES, solid-state nuclear magnetic resonance (SSNMR), and EPR. Byproduct shape selectivity of ZSM-48 in the SCWO of 2CP was also investigated.

Experimental Section

Experiments for catalytic SCWO of 2CP (Merck, purity >99.5%) were conducted in a high-pressure quartz-lined batch (volume = 20 mL) and an isothermal, isobaric fixed-bed reactor (volume = 14.85 mL) at 673 K for four minutes. The system pressure was controlled by a back-pressure regulator (Tescom, $P_{max} = 408$ atm) and a pressure regulator (Tescom, $P_{in} = 238$ atm; $P_{out} = 7$ atm). A safety rupture disk rated at 400 atm was installed. Concentrations of 2CP in the SCWO experiments were 1500 mg/L. Hydrogen peroxide (Merck, 30 wt %) was used as the oxidant (O/C ratio = 1.2) in the SCWO of 2CP.

Zeolite ZSM-48 (Si/Al = 350, Na/Al = 0.11) was synthesized from a reaction mixture containing fumed silica, 1,6-diaminohexane ((C_6DN), NaBr, and distilled water (detailed procedures described in refs 22 and 24). The CuO/ZSM-48 catalyst (Cu/Al = 0.56) was prepared by ion exchange of ZSM-48 in a 0.01 N $Cu(CH_3COO)_2$ aqueous solution for 24 h. The CuO/ZSM-48 catalyst was dried at 378 K for 16 h and calcined at 823 K for at least 6 h. About 2.4% of Cu was loaded on ZSM-48. The Si/Al ratio of ZSM-48 was determined by X-ray fluorescence (XRF, Rigaku model 3063M). The pore volume (0.15 mL g^{-1}) and surface area (900 m^2g^{-1}) of ZSM-48 were measured by nitrogen adsorption (Micromeritics ASAP 2010 instrument) and mercury penetration (Micromeritics Autopore II 9220), respectively.

Carbon dioxide produced from the SCWO of 2CP passed through a water cooler and was measured by a totalizer and analyzed by on-line FTIR spectroscopy and gas chromatography

10.1021/jp0043874 CCC: $20.00
Published on Web 05/05/2001

(GC) (Perkin-Elmer auto system). The GC was equipped with a thermal conductive detector (TCD) and a Supelco 60/80 Carboxen 1000 column (4.6 m in length, S. S.). Overall carbon balance for the SCWO of 2CP was > 95%. Infrared spectra were recorded on a Digilab FTIR spectrometer (FTS-40) with fully computerized data storage and data handling capability. For all spectra reported, a 64-scan data accumulation was conducted at a resolution of 4 cm^{-1}.

Trace byproducts (extracted with dichloromethane (Merck, purity > 99%)) formed in the SCWO of 2CP were determined quantitatively by GC (Hewlett-Packard 5890A) equipped with a mass selective detector (HP 5972) and an automatic sampler (HP-7673A). A HP Ultra 2 capillary column (50 m × 0.32 mm × 0.17 μm) was heated programmably (323 to 373 K at 20 K min^{-1}; 373 to 563 K at 3.5 K min^{-1}; and held at 563 K for 40 min) to obtain a resolvable separation of PAH species. The injection temperature was 583 K. Approximately 1to 2 μL of sample was injected into the column (HP Ultra 2 capillary column). Masses of primary and secondary ions of PAHs were determined using the scan mode for PAH standards (Mix 610-M (Supelco, purity > 99%) and PNA-550JM (Chem Service, purity > 99%)) and samples. The condensation byproducts were identified by searching and fitting the GC/MS library for compounds with similar mass spectra at a reliability over 90%. Analyses of trace byproducts of the SCWO of 2CP were also conducted by HPLC (spectra system, SP) with a 3-D UV detector (model UV-3000). PAHs were separated by a Spherisorb S5 PAH 5 μm column (150 mm × 4.6 mm) with a mixed acetonitrile/water mobile phase. Chlorinated phenols were analyzed by an Envirosep-PP column (125 mm × 3.2 mm) with a mixed methanol/water (both with 1% acetic acid) mobile phase. A variable wavelength program was used in the system software (model PC-1000) to optimize detector sensitivity and selectivity.

^{29}Si solid-state nuclear magnetic resonance (SSNMR) spectra of the catalysts were recorded at 9.4 T and 79.0 MHz on a Bruker Avance DSX 400 solid-state NMR spectrometer. Tetramethylsilane was used as a chemical shift reference (external standard) for ^{29}Si.[25−27] Bruker zirconia rotors (4 or 7 mm (o.d.)) were used and spun at a frequency of 5 kHz at the magic angle. Dry air was used as the driving and bearing gas in the SSNMR experiments. In all cases, a background signal was subtracted from the spectra. The recycle delay was 10 seconds with a pulse width of 3.0 μs (about 60° (flip angle)) for ^{29}Si.

The EXAFS and XANES spectra of the catalysts were recorded on the Wiggler BL17C beamline in the Taiwan Synchotron Radiation Research Center (SRRC). The electron storage ring was operated at an energy of 1.5 GeV (ring current = 100−200 mA). A Si(111) double-crystal monochromator (DCM) was used, and the energy resolution ($\Delta E/E$) of the beamline was about 1.9×10^{-4}. The X-ray absorption spectra were measured by a fluorescence detector (Lytle detector). The photon energy was calibrated against the adsorption edge of Cu foil at an energy of 8979 eV (Cu K edge). The standard deviation calculated from the averaged spectra was used to estimate the statistical noise and error associated with each structural parameter. The raw absorption data in the region of 50−200 eV were fit to a straight line using the least-squares algorithms. The fitted preedge background was extrapolated throughout the whole data range and subtracted and normalized to reduce effects of the sample thickness. The near-edge spectra were ranged between the threshold and the point at which the EXAFS began. The XANES spectra extend to an energy of 50 eV above the edge.[28−30] The Fourier transform was performed on k^2-weighted EXAFS oscillations in the range of 2.5 to 12 $Å^{-1}$. Multiple-shell fitting of the EXAFS data was conducted in R-space. The EXAFS data were analyzed using the UWXAFS 3.0 and FEFF 8.0 programs.[28−32]

TABLE 1: Trace PAH and Chlorinated Phenol Byproducts Formed in the SCWO of 2CP Catalyzed by CuO/ZSM-48 at 673 K for Four Minutes

		(μg (g 2CP)$^{-1}$)		
	min size[a] (Å)	no catalyst	ZSM-48	CuO/ZSM-48
S/D[b]		0.43	0.79	0.89
phenol	5.85	224.7	51.2	24.3
2,4-dichlorophenol	6.84	874.5	26.8	5.6
2,4.5- trichlorophenol	7.75	714.8	15.7	0.1
2,4,6-trichlorophenol	7.75	805.4	N. D.[c]	N. D.
2,3,4,6-tetrachlorophenol	7.75	154.2	N. D.	N. D.
pentachlorophenol	7.75	33.7	N. D.	N. D.
naphthalene	5.85	16.2	5.3	2.7
fluorene	5.85	1.6	0.9	0.5
phenanthrene	9.10	1.9	N. D.	N. D.
anthracene	5.85	2.0	0.7	0.2
pyrene	9.10	N. D.	N. D.	N. D.
benz[*a*]anthracene	9.10	1.1	N. D.	N. D.
chrysene	9.10	0.1	0.1	N. D.
benzo[*b*]fluoranthene	9.10	0.1	N. D.	N. D.
benzo[*a*]pyrene	9.10	0.2	N. D.	N. D.
dibenz[*a*,*h*]anthracene	9.45	N. D.	N. D.	N. D.
benzo[*ghi*]perylene	9.45	N. D.	N. D.	N. D.

[a] The minimum cross-section diameter.[22−24] [b] S/D = (amount of 2CP oxidized to CO_2 and H_2O)/(disappearance of 2CP). [c] N. D. denotes "not detectable".

The Cu(II) electron paramagnetic resonance (EPR) spectra of the catalysts were recorded on a Bruker Model EMX-10 EPR spectrometer with a maximum microwave power of 200 mW at 77−463 K. About 40−50 mg of the catalyst samples in the quartz tube (5 mm o.d.) was measured. The magnetic field was modulated at 100 kHz. Diphenylpicrylhydrazyl (DPPH) was used for determination of the absolute *g*-factor ($g = 2.0036$). All EPR spectra of the catalysts were normalized to the same frequency, sample weight, and spectrometer gain.[33−35] The EPR spectra could be compared by subtraction precisely and with accuracy of ±0.5%.

Results and Discussion

To obtain detectable quantities of incomplete oxidation compounds or byproducts in the SCWO of 2CP, we have intentionally conducted the experiments at temperatures somewhat less than 773 K (typically temperatures of 823−923 K are used for commercial applications of the SCWO process). A unique byproduct shape selectivity for oxidation of 2CP in supercritical water effected by CuO/ZSM-48 is shown in Table 1. Without the catalyst, 2,4-dichlorophenol and 2,4,5-trichlorophenol were the main chlorinated phenol byproducts formed in the SCWO of 2CP at 673 K for four minutes. Due to the confined environment in the channels of ZSM-48, Cl reinsertion may occur selectively at the energetically preferred sites (such as sites #4 and #5 (asterisk marked) in 2CP shown in Scheme 1). As expected, high Cl-substituted phenol byproducts such as 2,3,4,6-tetrachlorophenol and pentachlorophenol were not formed in the catalytic SCWO of 2CP in ZSM-48.

Furthermore, formation of heavy PAH byproducts in the catalytic SCWO of 2CP was also shape restricted in the channels of ZSM-48 (Table 1). Mainly low-molecular-weight PAHs such as naphthalene (NaP), fluorene (Flu), and anthracene (Ant) were formed in SCWO of 2CP. Carcinogenic PAHs including benzo[*a*]pyrene (BaP), benzo[*b*]fluoranthene (BbF), chrysene (CHR),

SCHEME 1[a]

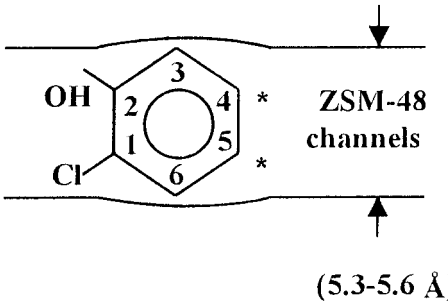

[a] Asterisk (*) denotes the possible Cl reinsertion sites of the tight-fit 2CP in the channels of ZSM-48.

SCHEME 2

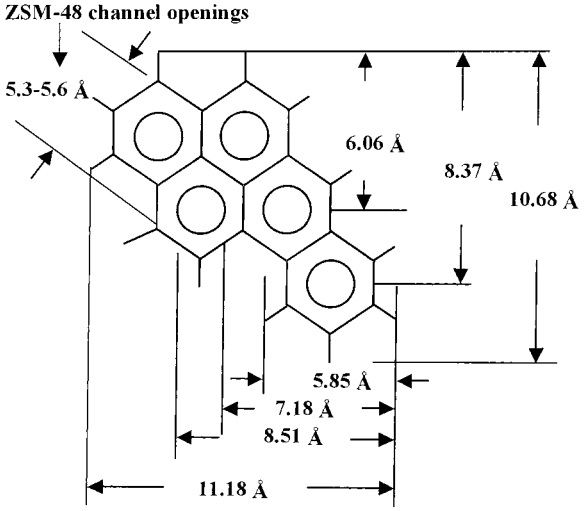

dibenz[*a*,*h*] anthracene (DBA), and benzo[*ghi*]perylene (BghiP) were not found in channels of ZSM-48 in the catalytic SCWO process (Scheme 2). Note that reactions of ring-opening in which products are ultimately oxidized to CO_2 and H_2O are predominant in the overall SCWO reaction.

To more thoroughly examine the nature of the active species involved in catalytic oxidation of 2CP in the channels of ZSM-48, XANES and EXAFS spectra of copper in ZSM-48 were studied (Figure 1). The XANES spectroscopy provides information of electronic configuration, stereochemistry, and the oxidation states of copper being investigated.[30−32] In Figure 1a, the preedge XANES spectrum of the CuO/ZSM-48 exhibits a very weak absorbance feature for the 1s-to-3d transition, which is forbidden by the selection rule in the case of perfect octahedral symmetry. The sharp feature at 8982−8983 eV, due to the dipole-allowed of electron transition of 1s-to-4p_{xy}, indicated the existence of Cu(I). The intensity of the 1s-to-4p_{xy} transition was proportional to the population of Cu(I) in ZSM-48. A shoulder at 8985−8986 eV and an intense feature at 8996−8998 eV were attributed to the 1s-to-4p_{xy} transition, which indicated the existence of Cu(II) species in the channels of ZSM-48. The upshift of the edge energy and a very weak absorption feature for 1s-to-3d forbidden transition near the preedge also confirmed the observations. The XANES spectra worked particularly well in distinguishing whether Cu(I) and Cu(II) coexisted in the channels of ZSM-48. In the SCWO process, we found that about 30% of the Cu(II) was reduced to Cu(I).

The main scientific issues concerning the chemical forms (or speciation) of active species ultimately depend on molecular-scale structure and properties. Basic understanding of this scale is essential for further understanding of the catalytic behaviors

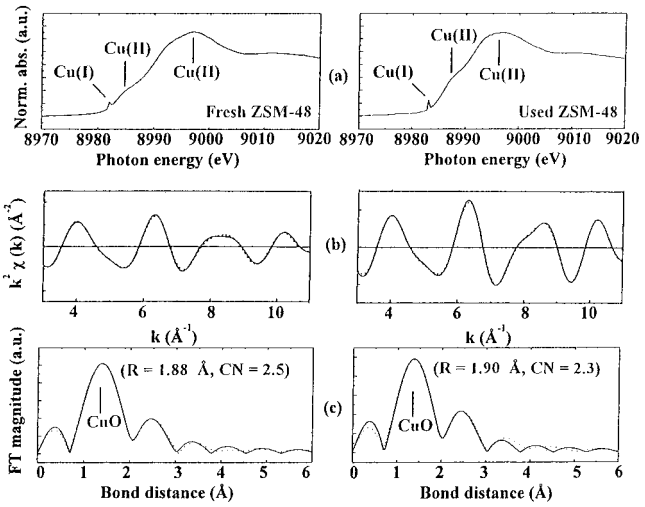

Figure 1. (a) XANES, (b) Cu K-edge EXAFS oscillation $k^2\chi$(k), and (c) Fourier transform (FT) of EXAFS $k^2\chi(k)$ of the fresh and used CuO/ZSM-48 catalysts in the SCWO of 2CP. The best fittings of the EXAFS spectra are expressed by the dotted lines.

TABLE 2: Structural Parameters of Copper Oxides in ZSM-48 in the SCWO of 2CP at 673 K for Four Minutes

	shell	CN[a]	R(Å)[b]	$\Delta\sigma^2$(Å^2)[c]
used CuO/ZSM-48				
Cu−O	1st	2.3	1.90	0.005
Cu−(O)−Cu	1st	4.1	2.80	0.008
fresh CuO/ZSM-48				
Cu−O	1st	2.5	1.88	0.003
Cu−(O)−Cu	1st	4.3	2.81	0.010
CuO				
Cu−O	1st	2.2	1.96	0.004
Cu−(O)−Cu	1st	4.3	2.91	0.007
Cu_2O				
Cu−O	1st	2.5	1.87	0.006
Cu−(O)−Cu	1st	3.1	12.5	0.019

[a] CN: Coordination number. [b] R: Bond distance (±0.05 Å). [c] s: Debye−Waller factor.

of copper oxide in ZSM-48. Generally, EXAFS spectroscopy can provide information on the atomic arrangement of catalysts in terms of bond distance, number and kind of near neighbors, and thermal and static disorders.[28−32] A reliability of the Fourier transformed EXAFS data fitting of more than 99% for Cu species in ZSM-48 was obtained (Figure 1c). Standard deviation calculated from the averaged spectra was also determined. In all EXAFS data analyzed, the Debye−Waller factors ($\Delta\sigma^2$) were less than 0.02 Å^{-1} (Table 2). The bond distances of Cu−O and Cu−(O)−Cu species were 1.90 and 2.80 Å, respectively. Coordination number (CN) for the Cu−O in the first shell was 2.3.

^{29}Si solid-state NMR spectra of the CuO/ZSM-48 catalyst used in the SCWO of 2CP are shown in Figure 2. The feature at −114 to approximately −103 ppm represents the Q_4 sites (Si(4Si, 0Al)), where all of the second-nearest-neighbor atoms were Si. Interactions of the copper species with the ═Si−O−Al═ sites on ZSM-48 seem to be insignificant. Copper-oxide species could be supported mechanically on ZSM-48.

Because the interactions between Cu and Si or Al were not observed by EXAFS and SSNMR, it is possible that copper oxide clusters with a cross-section of about 1.9 Å may be formed in the channels of ZSM-48. Due to the confined channels of ZSM-48 (5.5 Å), the basic units of the copper-oxide cluster that are involved in the SCWO of 2CP in the channels of ZSM-48 might be Cu_3O_2 (Scheme 3). In the SCWO process, the clusters

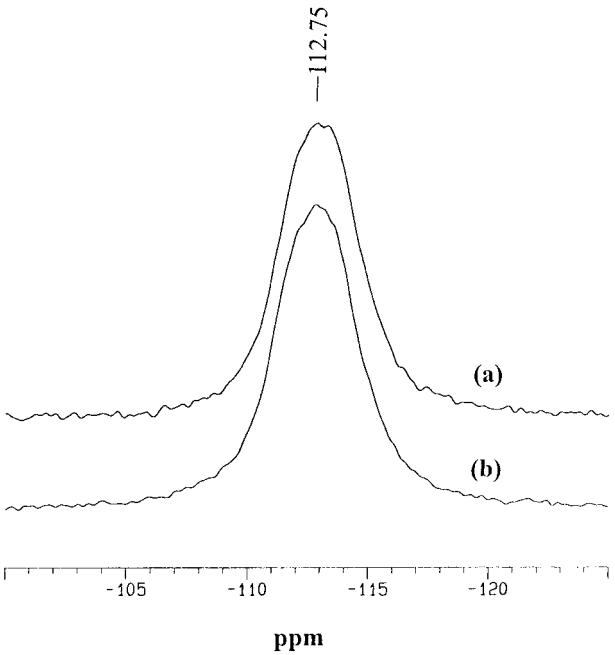

Figure 2. ^{29}Si SSNMR spectra of (a) fresh and (b) used CuO/ZSM-48 in the SCWO of 2CP.

SCHEME 3[a]

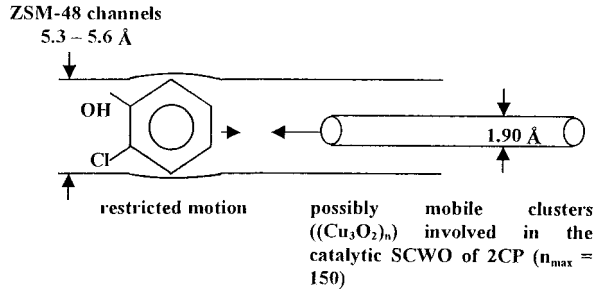

[a] The diffusion coefficient of $(Cu_3O_2)_n$ was greater than that of 2CP by at least three orders in the channels of ZSM-48

$((Cu_3O_2)_n)$ were partially oxidized by H_2O_2 with Cu−O and Cu−(O)−Cu bond distances of 1.88 and 2.81 Å, respectively.

In addition, electron paramagnetic resonance spectroscopy was also used to investigate the structural environment of the paramagnetic copper species in ZSM-48.[36−41] Determining the motion, location, and coordination of copper species in the channels of ZSM-48 is of great importance in understanding the role of copper species in the SCWO of 2CP. To study the behavior of the copper species in ZSM-48 for the SCWO of 2CP, the temperature dependence for the EPR (spin-Hamiltonian) parameters of copper was determined at 77−463 K (Table 3). The EPR spectra of the catalysts measured at 77, 298, and 463 K were fitted using the second-order perturbation equation and the least-squares polynomial fitting methods. The perpendicular components of g (effective Zeeman factor) and A (hyperfine coupling constant) for the individual signal could not be evaluated exactly because the signals were mostly overlaid and there was a lack of resolution in the split signal for CuO/ZSM-48.[37] Therefore, the parallel components of the axially symmetrical signals were used for the estimation of the Cu(II) coordination. The values of EPR parameters $g_{||} = 2.27-2.28$ and $A_{||} = 176-180$ G ($g_{||}$ and $A_{||}$ denote the g effective Zeeman factors and hyperfine coupling constants appropriate to the magnitudes $B_{||}$ of the magnetic field when it is parallel to the symmetry axis, respectively) of the catalysts were assigned

TABLE 3: Fitted EPR Parameters of Cu(II) for CuO/ZSM-48 Used in the SCWO of 2CP

temp (K)	$g_{||}$[a]	$A_{||}$[b] (G)	$g_{\perp}$[c]	$A_{\perp}$[d] (G)
77	2.28	176	2.06	20
298	2.27	179	2.06	21
463	2.27	180	2.05	23

[a,c] "$g_{||}$" and "$g_{\perp}$" denote the g effective Zeeman factors appropriate to the magnitudes $B_{||}$ and $B_{\perp}$ of the magnetic field when it is parallel and perpendicular to the symmetry axis, respectively. Estimated error of $g_{||}$ or $g_{\perp}$ is ± 0.01. [b,d] "$A_{||}$" and "$A_{\perp}$" denote the hyperfine coupling constants appropriate to the magnitudes $B_{||}$ and $B_{\perp}$ of the magnetic field when it is parallel and perpendicular to the symmetry axis, respectively. Estimated error of $A_{||}$ or $A_{\perp}$ is ± 5 G.

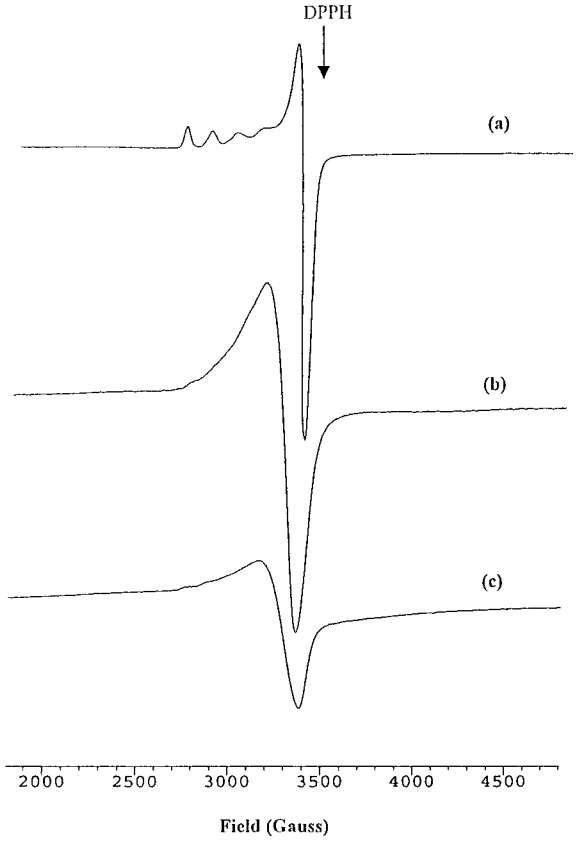

Figure 3. EPR spectra of the CuO/ZSM-48 catalysts used in the SCWO of 2CP measured at (a) 77, (b) 298, and (c) 463 K ($\nu_{EPR} = 9.784$ GHz, Field (Gauss) = 3476 or $g_{DPPH} = 2.0036$).

to the square-planar C_{4h} symmetry configurations with a higher copper content, and those of $g_{||} = 2.30-2.33$, $A_{||} = 150-160$ G were assigned to the square-pyramidal C_{4v} symmetry coordination with a low copper concentration. It seems that the copper species changed from the octahedral square-pyramidal to the planar coordination with the g-value decreasing and the hyperfine splitting tensor (A) increasing.

The spectra in regions of 2300 and 3800 G were integrated to obtain the intensities of the Cu(II) signals. Figure 3c shows that the EPR spectrum of the CuO/ZSM-48 catalyst (at 463 K) is broad and structureless, which may be caused by spin−lattice interaction between the Cu(II) and ZSM-48. On the contrary, at 77 K, the spectrum (Figure 3a) exhibits a sharp signal and characteristic structure of copper-oxide complexes. The hyperfine coupling between the 3d unpaired electrons and the copper nuclear spin quantum number (I) of 3/2 was well resolved.

Experimentally, the broad EPR spectrum observed at 463 K in Figure 3c suggests that the copper-oxide species may be mobile in the channels of ZSM-48. At 77 K, the appearance of

TABLE 4: Diffusion Coefficients of 2CP and Copper Oxide Clusters in the Channels of ZSM-48 in Supercritical Water

	$(Cu_3O_2)_{150}$	2-chlorophenol
molecular weight (g mol^{-1})	33397.5	128.56
L.-J. kinetic diameter (Å)	1.91	6.84
diffusion coefficient[a] (m^{2}s^{-1})	3.53×10^{-13}	3.20×10^{-16}

[a] Diffusion coefficients of 2CP and $(Cu_3O_2)_n$ (at 673 K) in the SCWO of 2CP were calculated using the equation: $D = kD_c(T/M)^{1/2}$ (where D_c is the channel factor depending on the zeolite pore sizes).[22−24,42−45]

the parallel edges in the EPR spectrum is observed in Figure 3a, which indicates a reduced mobility of copper species in ZSM-48 at low temperatures. The features in the low-field region of the EPR spectra shifted progressively when the catalyst was heated from 77 to 463 K. The observed changes in the EPR signal were reversible.

The postulated $(Cu_3O_2)_n$ cluster having a diameter of about 0.19 nm might be calculated from the square-planar structure observed by EXAFS spectroscopy. The ZSM-48 catalyst (with a unidimensional channel structure) used in the SCWO of 2CP consisted of rodlike crystals with an average length of 0.084 μm. The maximum n for $(Cu_3O_2)_n$ was about 150. The diffusion coefficient of the copper oxide-clusters ($(Cu_3O_2)_n$ with a minimum size of about 1.9 Å) was about 3.5×10^{-13} m^2 s^{-1} at 673 K in the channels of ZSM-48 calculated with the intensities of Cu EPR signals at 77−463 K (Table 4). Derived from the equation: $D = kD_c(T/M)^{1/2}$ (where D_c is the channel factor depending on the zeolite pore sizes (5.3−5.8 Å); $T = 673$ K; M is the molecular weight of 2CP (128.56 g mol^{-1}); and k is a parameter),[22−24] the diffusion coefficient of 2CP was about 3.20×10^{-16} m^2 s^{-1} in the tight-fit channel of ZSM-48. Therefore, the diffusion coefficient of the copper-oxide clusters was much greater than that of the tight-fit 2CP in the channel of ZSM-48 by at least three orders. The possible structures of the copper-oxide cluster and 2CP in the channels of ZSM-48 can, therefore, be described in Scheme 3. Because the SCWO of 2CP was extremely rapid (0.2 mM/s), we were forced to consider the possibility that the copper-oxide clusters $(Cu_3O_2)_n$ were relatively mobile during the SCWO of 2CP in the channels of ZSM-48.

Conclusions

A unique byproduct shape selectivity for limiting the formation of carcinogenic PAHs and chlorinated phenol byproducts in SCWO of 2CP effected by CuO/ZSM-48 was observed. The copper oxides in the channels of ZSM-48 possess Cu−O and Cu−(O)−Cu bond distances of 1.90 and 2.80 Å, respectively. The diffusion coefficient of copper oxides was greater than that of 2CP in the channels of ZSM-48 by at least three orders. Because the catalytic SCWO of 2CP was extremely rapid, it is possible that the copper oxides might be relatively mobile (compared with 2CP) in the confined channels of ZSM-48 for the SCWO of 2CP. This work demonstrated the usefulness of EXAFS and XANES in revealing the speciation of copper oxides, specifically a possibly mobile active center, in the confined channels of ZSM−48 for the SCWO of 2CP.

Acknowledgment. The financial support of the National Science Council, Taiwan is gratefully acknowledged. We also thank Prof. Y. W. Yang and Dr. J. F. Lee of the Taiwan Synchrotron Radiation Research Center for their help in the EXAFS experiments and Ms. Ru-Rong Wu of the National Cheng Kung University for her SSNMR experimental assistance.

References and Notes

(1) Kaune, A.; Lenoir, D.; Schramm, K. W.; Zimmermann, R.; Kettrup, A.; Jaeger, K.; Ruckel, H. G.; Frank, F. *Environ. Eng. Sci.* **1998**, *15*, 85−95.

(2) Thornton, T. D.; LaDue D. E., III; Savage, P. E. *Environ. Sci. Technol.* **1991**, *25*, 1507−1510.

(3) Wang, H. P.; Hsieh, K. A.; Li, M. C. *J. Environ. Sci. Health* **1997**, *A32*, 1687−1694.

(4) Bjørseth, A. *Handbook of Polycyclic Aromatic Hydrocarbons*, 2nd ed.; Marcel Dekker: New York, 1983; pp 34−65.

(5) Yasuda, K.; Takahashi, M. *J. Air Waste Manage. Assoc.* **1998**, *48*, 441−447.

(6) Lin, K. S.; Wang, H. P. *Environ. Sci. Technol.* **2000**, *34*, 4849−4854 and references therein.

(7) Lin, K. S.; Wang, H. P. *Appl. Catal. B: Environ.* **1999**, *22*, 261−267. Lin, K. S.; Wang, H. P. *Environ. Sci. Technol.* **1999**, *33*, 3278−3280. Lin, K. S.; Wang, H. P. *Langmuir* **2000**, *16*, 2627−2631.

(8) Fernàndez, D. P.; Goodwin, A. R. H.; Lemmon, E. W.; Levelt Sengers, J. M. H.; Williams, R. C. *J. Phys. Chem. Ref. Data* **1997**, *26*, 1125−1166.

(9) Modell, M. In *Standard Handbook of Hazardous Waste Treatment and Disposal*; Freeman, H. M., Ed.; McGraw-Hill: New York, 1989; sec. 8.11, pp 153−168.

(10) Li, R.; Savage, P. E.; Szmukler, D. *AIChE J.* **1993**, *39*, 178−187.

(11) Savage, P. E.; Smith, M. A. *Environ. Sci. Technol.* **1995**, *29*, 216−221.

(12) Kronholm J.; Riekkola M. L. *Environ. Sci. Technol.* **1999**, *33*, 2095−2099.

(13) Anitescu, G.; Tavlarides L. L. *Ind. Eng. Chem. Res.* **2000**, *39*, 583−591.

(14) Martino, C. J.; Savage, P. E. *Environ. Sci. Technol.* **1999**, *33*, 1911−1915; *38*, 1784−1791.

(15) Ding, Z. Y.; Aki, S. N. V. K.; Abraham, M. A. *Environ. Sci. Technol.* **1995**, *29*, 2748−2753.

(16) Aki, S. N. V. K.; Abraham, M. A. *Ind. Eng. Chem. Res.* **1999**, *38*, 358−367.

(17) Zhang, X.; Savage, P. E. *Catal. Today* **1998**, *40*, 333−342.

(18) Oshima, Y.; Tomita, K.; Koda, Seiichiro, S. *Ind. Eng. Chem. Res.* **1999**, *38*, 4183−4188.

(19) Yu, J.; Savage, P. E. *Ind. Eng. Chem. Res.* **1999**, *38*, 3793−3801.

(20) Alejandre, A.; Medina, F.; Fortuny, A.; Salagre, P.; Sueiras, J. E. *Appl. Catal. B: Environ.* **1998**, *16*, 53−67.

(21) Oshima, Y.; Hori, K.; Toda, M.; Chommanad, T.; Koda, S. *J. Supercrit. Fluids* **1998**, *13*, 241−246.

(22) Chu, P. European Patent 23,089, 1980; U.S. Patent 4,397,827, 1981; U.S. Patent 4,397,827, 1983; U.S. Patent 4,448,675, 1984.

(23) Breck, D. W. *Zeolite Molecular Sieves*, 1st ed.; John Wiley & Sons: New York, 1974; pp 634−642.

(24) Wang, H. P.; Lin, K. S.; Huang, Y. J.; Li, M. C.; Tsaur, L. K. *J. Hazardous Mater.* **1998**, *58*, 147−152.

(25) Hu, S.; Reimer, J. A.; Bell, A. T. *J. Phys. Chem. B* **1997**, *101*, 1869−1871.

(26) Hunger, M. *Catal. Rev.- Sci. Eng.* **1997**, *39*, 345−393.

(27) Dybowski, C. *Anal. Chem.* **1998**, *70*, 1R-5R.

(28) Zabinsky, S. I.; Rehr, J. J.; Ankudinov, A.; Albers, R. C.; Eller, M. J. *Phys. Review B−Condens. Matter* **1995**, *52*, 2995−3001.

(29) Resslert, T. *J. Synchrotron Rad.* **1998**, *5*, 118−122.

(30) Korshin, G. V.; Frenkel, A. I.; Stern, E. A. *Environ. Sci. Technol.* **1988**, *22*, 2699−2705.

(31) Vlaic, G.; Andreatta, D.; Colavita, P. E. *Catal. Today* **1998**, *14*, 261−275.

(32) Koningsberger, D.; Mojet, B.; Miller, J.; Ramaker, D. *J. Synchrotron Rad.* **1999**, *6*, 135−141.

(33) Hoffmann, M. M.; Darab, J. G.; Palmer, B. J.; Fulton, J. L. *J. Phys. Chem. A* **1999**, *103*, 8471−8482.

(34) Kumashiro, R.; Kuroda, Y.; Nagao, M. *J. Phys. Chem. B* **1999**, *103*, 89−96.

(35) Kucherov, A. V.; Slinkin, A. A.; Kongratev, D. A.; Bondarenko, T. N.; Rubinstein, A. M.; Minachev, Kh. M. *Zeolites* **1985**, *5*, 320−323.

(36) Dědeček, J.; Sobalík, Z.; Tvaruzková, D.; Kaucky, B.; Wichterlovà, B. *J. Phys. Chem.* **1994**, *99*, 16327−16331.

(37) Weil, J. A.; Bolton, J. R.; Wertz, J. E. *Electron Paramagnetic Resonance- Elementary Theory and Practical Applications*; John Wiley & Sons: New York, 1994; pp 294−333.

(38) Anderson, M. W.; Kevan, L. *J. Phys. Chem.* **1987**, *91*, 4174−4179.

(39) Kucherov, A. V.; Slinkin, A. A. *Kinet. Catal.* **1997**, *38*, 1−7.

(40) Dyrek, K.; Adamski, A.; Sojka, Z. *Spectrochim. Acta, Part A* **1998**, *54*, 2337−2348.

(41) Patrick, J.; Larsen, S. C. *J. Catal.* **1999**, *182*, 208−218.

(42) Schlenker, J. L.; Rohrbaugh, W. J.; Chu, P.; Valyocsik, E. W.; Kokotailo, G. T. *Zeolites* **1985**, *5*, 355−358.

(43) Choudhary, V. R.; Singh, A. P. *Zeolites* **1986**, *6*, 206−208.

(44) Hayhurst, D.; Paravar, A. R. *Zeolites* **1988**, *8*, 27−29.

(45) Garcia, S. F.; Weisz, P. B. *J. Catal.* **1990**, *121*, 294−311.